Interannual variability and ventilation timescales in the ocean cavity beneath Filchner-Ronne Ice Shelf, Antarctica

K. W. Nicholls
British Antarctic Survey, Natural Environment Research Council, Cambridge, UK

S. Østerhus
Bjerknes Centre for Climatic Research, University of Bergen, Bergen, Norway

Received 30 September 2003; revised 12 February 2004; accepted 25 February 2004; published 20 April 2004.

[1] Multiyear time series of ocean current and temperatures from beneath Filchner-Ronne Ice Shelf, Antarctica, demonstrate both seasonal and interannual variability. The seasonal signal is visible at all measurement sites, although it was swamped for a 2-year period (1999–2001) when extraordinarily light sea-ice cover in the southern Weddell Sea during the 1997–1998 Austral summer caused an anomalously large pulse of High Salinity Shelf Water to flush beneath the ice shelf. The pulse was observed twice at an instrumented site near the Berkner Island coast, once on its way to the Filchner Depression and once after the signal had propagated around the depression and returned to the site as an anomalously large pulse of Ice Shelf Water. The timings of the signal allow an estimate of 24–30 months for the flushing timescales of the sub-ice shelf ocean cavity, indicating that the cavity is highly responsive to external forcing. A timescale for the full ventilation of the cavity of 4–5 years is obtained from the length of time the sub-ice shelf conditions take to return to their original state, a timescale significantly shorter than previous estimates. *INDEX TERMS:* 4207 Oceanography: General: Arctic and Antarctic oceanography; 9310 Information Related to Geographic Region: Antarctica; 4283 Oceanography: General: Water masses; *KEYWORDS:* interannual variability, ice shelf, Antarctica

Citation: Nicholls, K. W., and S. Østerhus (2004), Interannual variability and ventilation timescales in the ocean cavity beneath Filchner-Ronne Ice Shelf, Antarctica, *J. Geophys. Res.*, *109*, C04014, doi:10.1029/2003JC002149.

1. Introduction and Geophysical Setting

[2] Weddell Sea Bottom Water (WSBW) is a precursor of the Antarctic Bottom Water produced in the Weddell Sea sector of the Antarctic and has its origins over the Weddell Sea continental shelf (Figure 1). Sea ice formation over the continental shelf, and export of that sea ice to the north, generates High Salinity Shelf Water (HSSW). HSSW is the densest water mass on the continental shelf as, in the Antarctic seas, changes in salinity rather than temperature dominate the variation in density. WSBW is produced when HSSW descends the continental slope after either flowing directly to the shelf break [*Foster and Carmack*, 1976], or by first being modified by interaction with glacial ice. WSBW formed by processes involving glacial ice has properties slightly different to those of WSBW formed without interaction with glacial ice [*Gordon*, 1998].

[3] Processes beneath Filchner-Ronne Ice Shelf (FRIS) are thought to affect the flux and properties of WSBW. By volume the largest Antarctic ice shelf, the FRIS occupies around 450,000 km^2 of the continental shelf in the southern Weddell Sea. A program of research has been running since the early 1980s to study the interaction between the FRIS and the underlying waters. The research has comprised the development of numerical models of the interaction between ice shelf and ocean [*Williams et al.*, 1998; *Jenkins and Holland*, 2002; *Jenkins et al.*, 2004]; oceanographic cruises over the continental shelf north of the ice front (the seaward edge of the ice shelf) [e.g., *Gammelsrød et al.*, 1994]; glaciological studies of the impact of the ocean on the ice shelf [e.g., *Jenkins and Doake*, 1991]; and direct measurements of the regime within the sub-ice shelf cavity via hot water drilled access holes [*Nicholls and Makinson*, 1998; *Nicholls et al.*, 2001]. In addition, a small number of oceanographic moorings have been recovered from near Ronne Ice Front, yielding estimates of HSSW fluxes into the sub-ice shelf cavity [*Foldvik et al.*, 2001; *Nicholls et al.*, 2003].

[4] One result of the research has been the demonstration that the principal external oceanographic forcing on the sub-ice shelf cavity is the production of HSSW during the Austral winter [*Nicholls*, 1996]. The inset diagram in Figure 1 shows a simplified schematic cross section of the ice shelf. The full three dimensional circulation is clearly more complicated, but the diagram serves to illustrate the principal processes. A key topographic feature of the southern Weddell Sea continental shelf is the way the seafloor beneath the FRIS deepens toward the grounding line, where the ice shelf goes afloat. This enables HSSW

0148-0227/04/2003JC002149$09.00

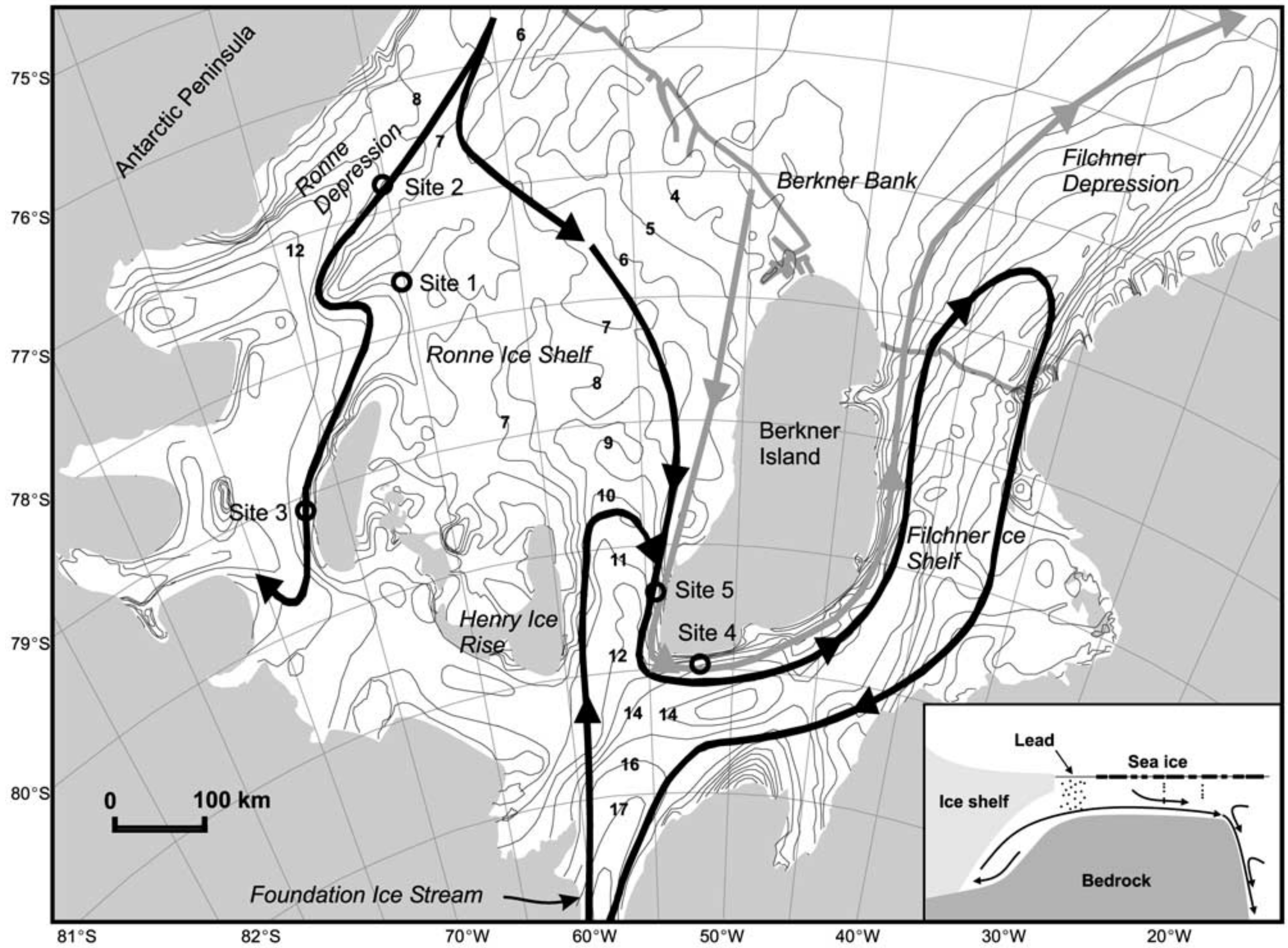

Figure 1. Map showing the Filchner-Ronne Ice Shelf in the southern Weddell Sea. The contours are of bathymetry with a separation of 100 m, and are labeled in 100s of meters. Arrows show principal flows beneath the ice shelf. The inset diagram shows a schematic cross section of the ice shelf, indicating production of HSSW seaward of the ice front, sinking of the HSSW beneath the ice shelf, and conversion of the HSSW into ISW by interaction with the ice shelf base.

produced north of the ice front to drain into the cavity under gravity, thus providing an externally driven circulation. HSSW is at or near the surface freezing point, but, because of the depression of the freezing point of seawater with pressure [*Millero*, 1978], the HSSW that flows beneath the ice shelf has the capacity to melt ice at the depth of the interface between ice shelf and ocean. HSSW that has been cooled by this interaction with the ice shelf base is below the surface freezing point ($\sim -1.9^\circ$C), and is called Ice Shelf Water (ISW). In the southern Weddell Sea an ISW-rich plume is observed overflowing the shelf break and descending to the depths, where it contributes to the formation of WSBW [*Foldvik and Gammelsrød*, 1988].

[5] Internal gyre-type circulations are thought to occur in combination with the externally driven flow [*Gerdes et al.*, 1999]. The internally driven circulation is powered by the difference in freezing point between the base of the ice shelf at the deep grounding lines, and the shallower ice base toward the ice front. As the relatively buoyant, but very cold ISW ascends the ice shelf base, the decrease in pressure can cause the ISW to become in situ supercooled. Ice crystals then form in the ISW plume, maintaining the temperature near the local pressure freezing point and increasing the bulk plume buoyancy. When the crystals rise to the ice base the decrease in buoyancy of the ISW, coupled with the local topography, can cause the flow to return to the grounding line where it is able to melt more ice. This internal type of circulation would be expected to be largely independent of variability north of the ice front.

[6] The externally driven circulation depends on the production of sea ice, and so has a strong seasonal component. This is illustrated in Figure 2, which shows a 3-year time series of temperatures recorded at site 3 (Figure 1). The series has been filtered with a cutoff at 100 days to highlight the annual cycle, which is a result of variations in the thickness of an HSSW-rich layer at the bottom of the water column [*Nicholls*, 1996].

[7] In total, five oceanographic sites have been occupied across the ice shelf, each of which has supplied a sequence of conductivity-temperature-depth (CTD) profiles, and longer-term time series of temperatures and/or water currents. More recently, a further four sites have been occupied toward the north of the ice shelf, though these

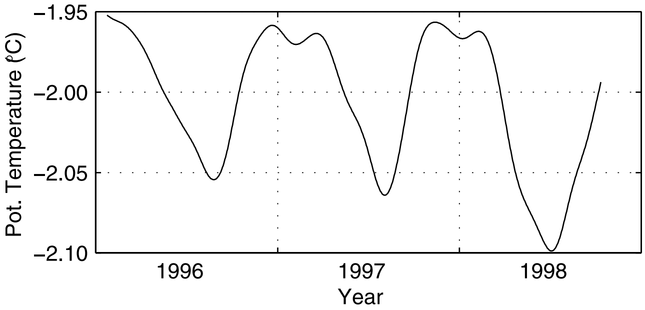

Figure 2. The temperature signal from a sensor 220 m above the seafloor and 270 m below the ice base at site 3. The data have been low-pass filtered with a cutoff period of 100 days.

have not yet supplied time series of significant length. Figure 1 shows a simplified schematic of the circulation paths that have been deduced from a combination of measurements made at the five ice shelf sites, ship-based measurements made along the ice front, and glaciological measurements of the ice shelf itself. In this paper we present new time series of temperature and velocity from site 5. The time series from site 5 are over 4 years long, and give an indication of seasonal and interannual variability at its location near the coast of the southern tip of Berkner Island (Figure 1). In section 2 we describe the moorings and the sites themselves, we show how the longer time series now available modify our model of the oceanographic regime at site 5, and we discuss the long-term variability visible in the data. In section 3 we suggest a source for the interannual variability observed at site 5. An estimate of the timescales for ventilating the sub-ice shelf cavity is presented in section 4.

2. Time Series From Site 5

[8] Sites 4 and 5 were established in January 1999. Site 4 was located 12 km south of Berkner Island (S80° 59′.1, W051° 36′.4); site 5 was 17 km west of the south-western coast of Berkner Island (S80° 20′.0, W054° 46′.4) (Figure 1). All instruments except the deep current meter at site 4 supplied time series, though the deep current meter at site 5 failed after only 143 days. The longest records are from site 5, and for the purposes of this paper, which is principally focused on interannual variability, those are the records with which we will be mainly concerned. Figure 3 [from *Nicholls et al.*, 2001] shows the profiles of mean potential temperature (θ) and salinity (S) that were obtained from site 5 when the site was established, together with the depths of the moored instruments.

[9] With the exception of the deep current meter at site 4, all current meters used the Aanderaa DCS3900 Doppler current head, the same unit as used in the RCM9 current meter. The temperature and conductivity sensors were also Aanderaa units. The temperature sensors and, in particular, the conductivity sensors suffered from rather low resolution, and the conductivity sensors generally showed a serious initial relaxation that took several weeks to settle. As a result, the TC units were unable to provide absolute values of salinity. The resolution and estimated accuracy of the temperature sensors is 0.005°C and ±0.01°C, respectively.

[10] *Nicholls et al.* [2001] set the CTD data obtained from the two sites in the context of the data available from north of the ice front and the topography of the sub-ice shelf cavity. Their main conclusion was that there exist two distinct circulations, as indicated in Figure 1. The first is driven by a combination of drainage beneath the ice shelf of dense HSSW from the western end of Ronne Ice Front, and the transfer of basal ice from deep to shallower drafting regions of the ice shelf, principally northeast of Henry Ice Rise (Figure 1). The latter process is often referred to as an "ice pump". This circulation occupies the deeper parts of the cavity, and, in unmodified form, the water is too dense to escape the Filchner Depression, but recirculates beneath the ice shelf. Such a recirculation of dense ISW has been previously proposed by *Carmack and Foster* [1975] and *Foldvik et al.* [1985] using ship-based observations obtained from the open Filchner Depression. The second circulation is driven by a lower salinity, and therefore less dense version of HSSW formed over Berkner Bank at the eastern end of Ronne Ice Front (Figure 1). As it flows around Berkner Island this lower-density water interacts with the ice shelf base. The resulting ISW traverses the western slope of the Filchner Depression and flows over the sill that is formed by the intersection of the depression with the continental shelf break. We assume that the denser, topographically trapped, recirculating ISW is ultimately converted to a form light enough to surmount the sill and escape the Filchner Depression along with its counterpart originating from Berkner Bank, though we have no evidence for how the conversion is performed. The CTD

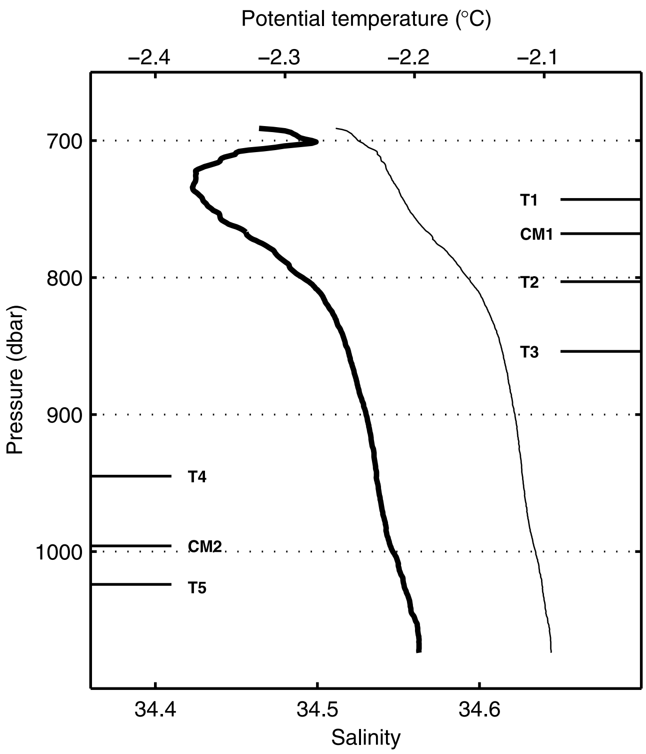

Figure 3. Mean potential temperature and salinity (fine line) profiles from the CTD data obtained at site 5, with the locations of conductivity-temperature (T) and current meter (CM) instruments indicated.

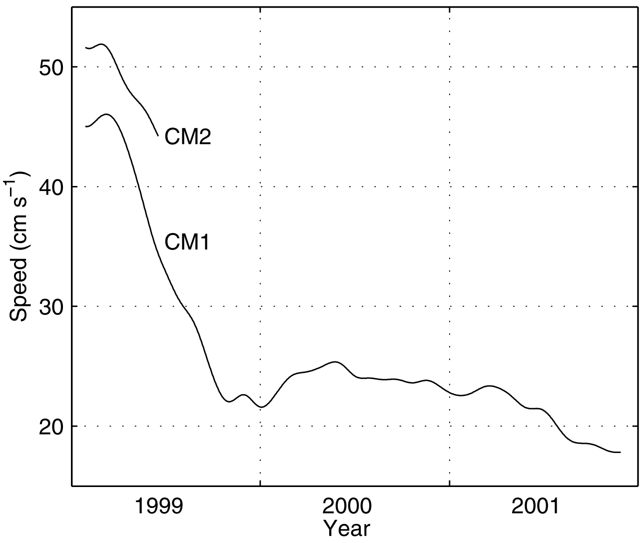

Figure 4. Time series of along-mean flow speeds measured at site 5. The data have been low-pass filtered with a cutoff at 100 days.

profiles revealed a warm layer near the ice base at site 5 (Figure 3). *Nicholls et al.* [2001] interpret this as having come from the lower-density Berkner Bank inflow that lies between the site 5 and the coast, some of which has been advected to the west within the Ekman layer, and therefore made visible near the ice base at site 5. They show that the remainder of the water column sampled at that time (at the beginning of the time series) originated from the denser, western inflow, and from water recirculating from the freezing area near Henry Ice Rise (Figure 1).

[11] The time series from the current meters at site 5 are shown in Figure 4. To highlight the longer-term variability with which this paper is primarily interested, the data have been low-pass filtered with a cutoff of 100 days. The velocities have been resolved along the mean flow vector for each instrument. On the basis of the few months of time series available at that time, and by analogy with the records from the Ronne Depression (Figure 2, for example) *Nicholls et al.* [2001] concluded that the rapid decrease in speed of flow in the record was the result of a seasonal change. They suggested that the flow from Berkner Bank increased as the sea-ice production season was entered, displacing the flow to the west and enveloping the site 5 mooring. The flow from the Berkner Bank would therefore have to have been fast compared with the flow farther to the west.

[12] Figure 5 (top) shows the potential temperature (θ) time series for each of the temperature sensors at site 5. The records have again been low-pass filtered with a cutoff of 100 days. The longer records now available show very clearly that, for the first half of the record the variability is not strongly seasonal in the upper half of the water column, and is different to the variability observed in the Ronne Depression. However, the conclusion that during the first 10 months of the record, the principal influence on the water column at site 5 switches from the colder inflowing and recirculating waters from the west, to the warmer inflow along the Berkner coast is consistent with the longer temperature time series. There is an obvious overall warming in the water column during the first 10 months of the time series, during which time the upper part of the water column becomes more uniform in temperature. The nature of the warming is best seen in the unfiltered temperature data, the first ten months of which are shown in Figure 5 (bottom) for the shallowest (coldest) sensor. Here we see that the temperature exhibits a marked variability on timescales of the order of days, with the water appearing to move between warm and cold modes, the mean temperature depending on the time spent in each mode. The temperature difference between each mode is approximately 0.15°C, which corresponds to the difference observed in the CTD profiles between the warm water of Berkner Bank origin, seen in the upper boundary layer, and the colder water just below (Figure 3).

[13] The schematic in Figure 6 gives a plausible configuration of isotherms that explains the CTD data, and is consistent with the current meter data. The ice shelf draft and seafloor depth were obtained from seismic data [*Nicholls et al.*, 2001]. The arrangement of isotherms shown in the figure corresponds to the conditions at the start of the time series, with the flow from the Berkner Bank (BB) confined to the vicinity of the Berkner coast, and with only a trace visible at site 5 within the upper boundary layer. The deepest layer is fed by the inflow from the Ronne Depression (RD), while the intermediate layer is from the water that recirculates from the freezing zone northeast of

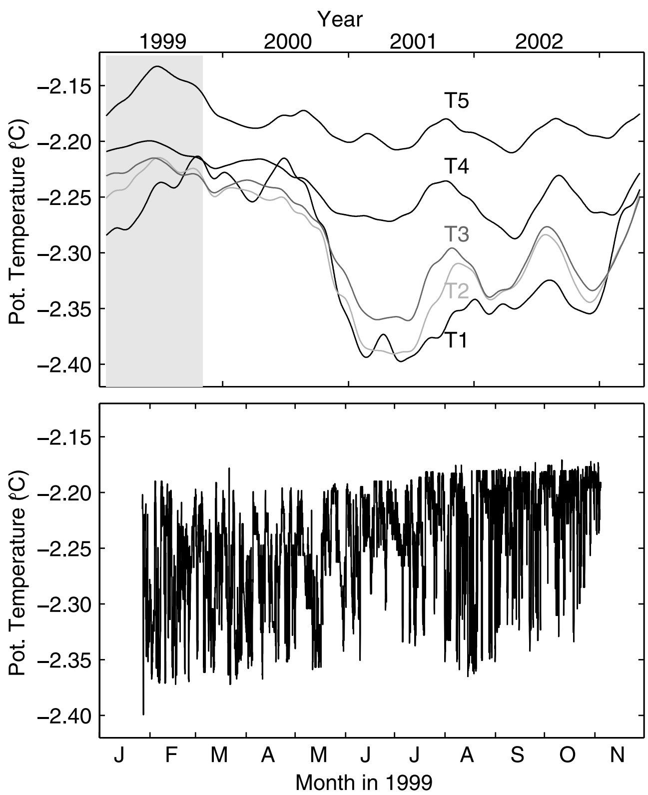

Figure 5. (top) The potential temperature time series from the temperature sensors at site 5, filtered with a cutoff at 100 days. The shaded band indicates the time interval displayed in Figure 5 (bottom), which shows the first 10 months of the unfiltered record from the uppermost temperature sensor.

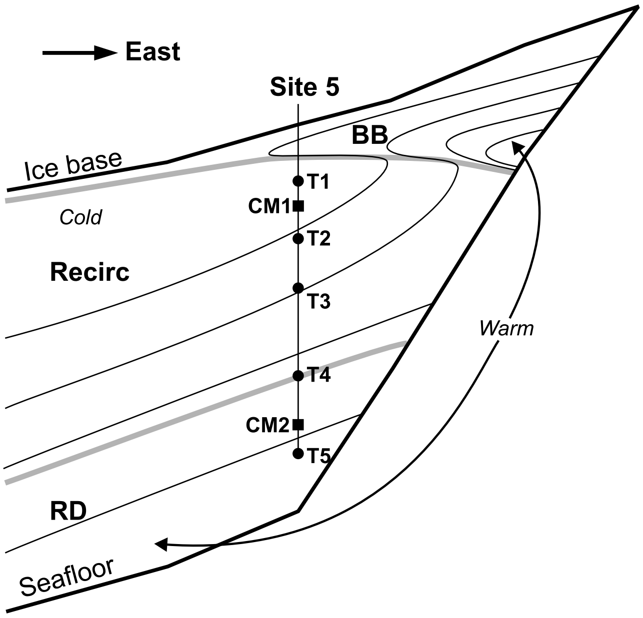

Figure 6. Schematic of isotherms (fine black lines) in an east-west section (looking north) from Berkner coast through site 5. Berkner Island is to the right. Broad shaded lines are isopycnals separating BB (water from Berkner Bank) from recirculating water and RD (water from Ronne Depression). The schematic corresponds to the time when the CTD profiles were obtained (late summer). Circles and squares indicate the locations of the temperature sensors and current meters, respectively.

Henry Ice Rise (Figure 1). For this configuration to be geostrophically consistent, both the inflowing RD water in the deep part of the water column and the inflowing BB water must be flowing faster than the intermediate depth recirculating water. The current meter records (Figure 4) confirm that the inflowing RD water is flowing faster than the recirculating water above. The arrangement of isotherms is consistent with the notion that, as the winter progresses, the BB flow increases, gradually pushing the isotherms to the west, and raising the temperature of the entire water column observed at site 5. There are other possible interpretations, but the configuration suggested in Figure 6 has the merit of being relatively simple while remaining consistent with our (admittedly limited) data set.

[14] The contour plot in Figure 7 shows the evolution of the temperature within the subice cavity at site 5. It shows a dramatic cooling in the upper half of the water column, starting around October 2000, and lasting for about 11 months. Where does this cold water originate? A study of the unfiltered time series shows that the lowest temperature attained during this period was recorded by the upper CT unit, and was −2.435 ± 0.01°C. To attain a temperature this low, the water must have interacted with a deeply drafting part of the ice shelf. A minimum value for this draft can be found by calculating the pressure required to depress the freezing point to the minimum observed temperature. The freezing point also depends on salinity, an estimate of which can be obtained from inspection of the θ-*S* plot for the CTD data from site 4 [*Nicholls et al.*, 2001]. An in situ temperature of −2.435 ± 0.01°C (θ = −2.451 ± 0.01°C) corresponds to a salinity of 34.53, with a likely error of about 0.02. We therefore calculate a minimum draft of between 700 and 730 dbar. The draft at site 5 is 685 dbar. ISW of such a low temperature must therefore have been formed in a region to the west and south of site 5 where the draft of the ice shelf is greater. This is consistent with the ISW glut having been formed east of Henry Ice Rise, and then recirculating to site 5 (Figure 1). Under this interpretation, in October 2000 the upper half of the site 5 water column reverts to being influenced by recirculating water. Although this change is not reflected in the magnitude of

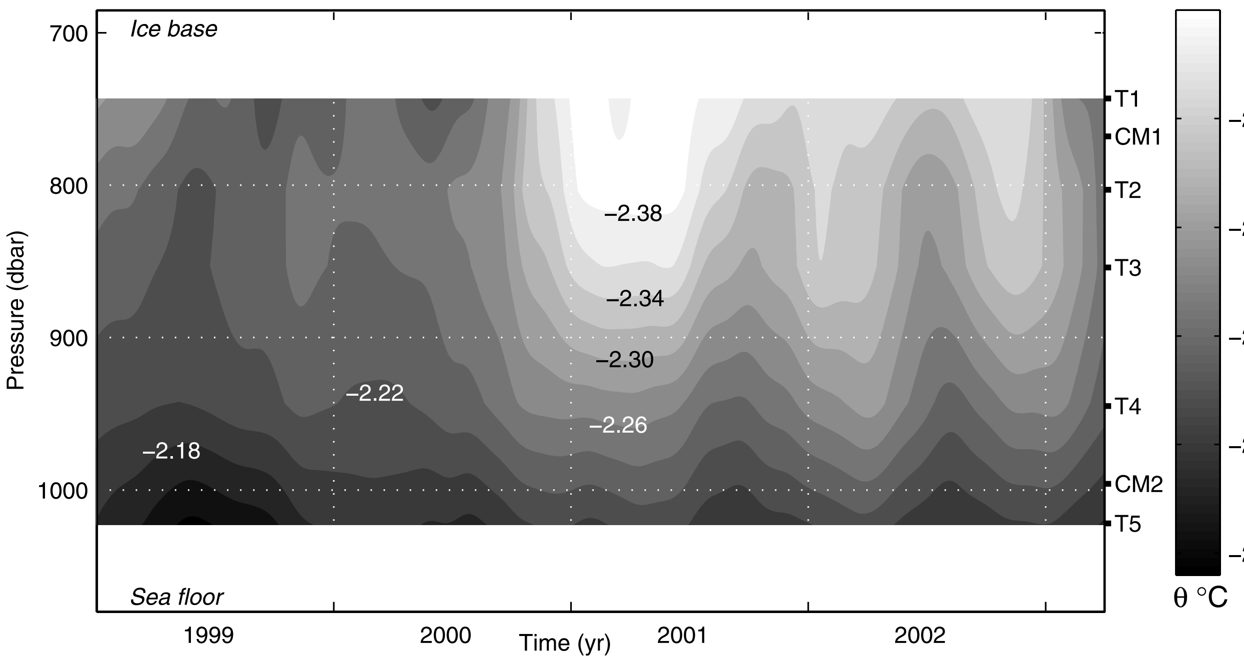

Figure 7. Contour plot showing evolution of potential temperature at site 5.

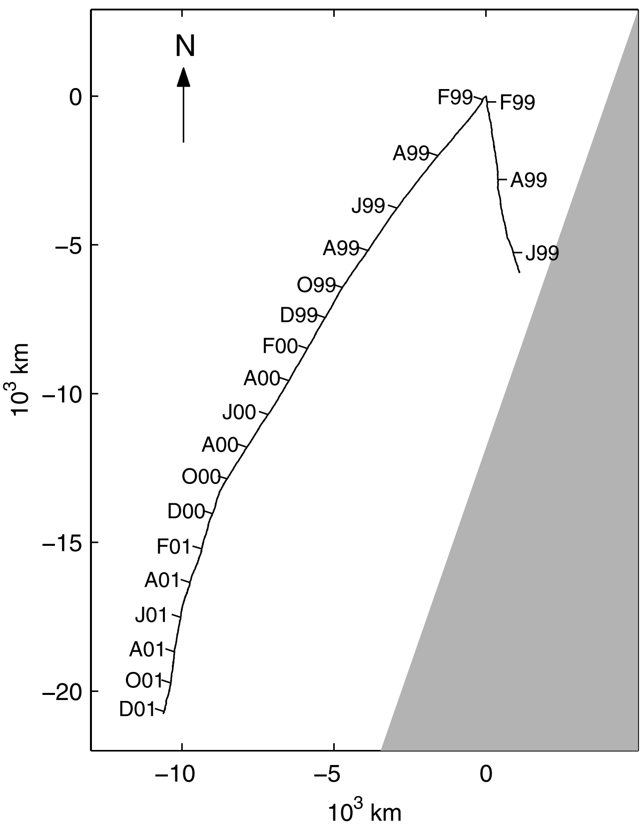

Figure 8. Progressive vector diagrams for site 5 current records. The shaded area indicates the orientation of the Berkner Island coast.

the along-flow component of the current measured by the upper current meter (Figure 4), it can be seen in the direction of flow, which swings further toward the south, as illustrated by the progressive vector diagrams shown in Figure 8.

[15] During the following 18 months the upper half of the water column displays a gradual recovery to higher temperatures, superimposed on an annual signal. The deeper water column recovers more rapidly, with an undisturbed seasonality visible from mid-2001. We expect the seasonality in the temperature signal to be dominated by advection of temperature gradients (both horizontal and vertical) past the instruments. The vertical temperature gradients are substantially lower prior to 2001 (Figure 7), helping explain the weak or absent seasonal signal above the deepest sensor.

3. Source of Variability

[16] The marked interannual variability visible in the records from site 5 can only be explained by variability in processes north of the ice front. During the Austral summer a polynya generally opens up at the FRIS ice front [*Renfrew et al.*, 2002]. The extent of the polynya is variable, but is often as narrow as a few kilometers. With the onset of winter the polynya closes up, but a combination of winds and tidal action serves to maintain shore leads along the ice front. The early winter freeze-up of the polynya deposits a pulse of salt into the upper water column, the size of which depends on the area of open water available at the end of the summer and the process by which the polynya was formed. If the polynya was formed by in situ melting of sea ice, the subsequent freeze-up will produce no net increase in salinity. HSSW will be produced, however, if the polynya had formed as a result of wind-forced advection of sea ice from the continental shelf.

[17] During the Austral summer of 1997–1998 a polynya of extraordinary area developed, extending from the ice front to the continental shelf break (Figure 9) [*Hunke and Ackley*, 2001]. The extent of the polynya was unprecedented during the satellite era, and has not been repeated since. *Ackley et al.* [2001] found that the extensive open water area was a result of anomalously high southerly and southwesterly winds during the 1997–1998 Austral spring and summer, thus

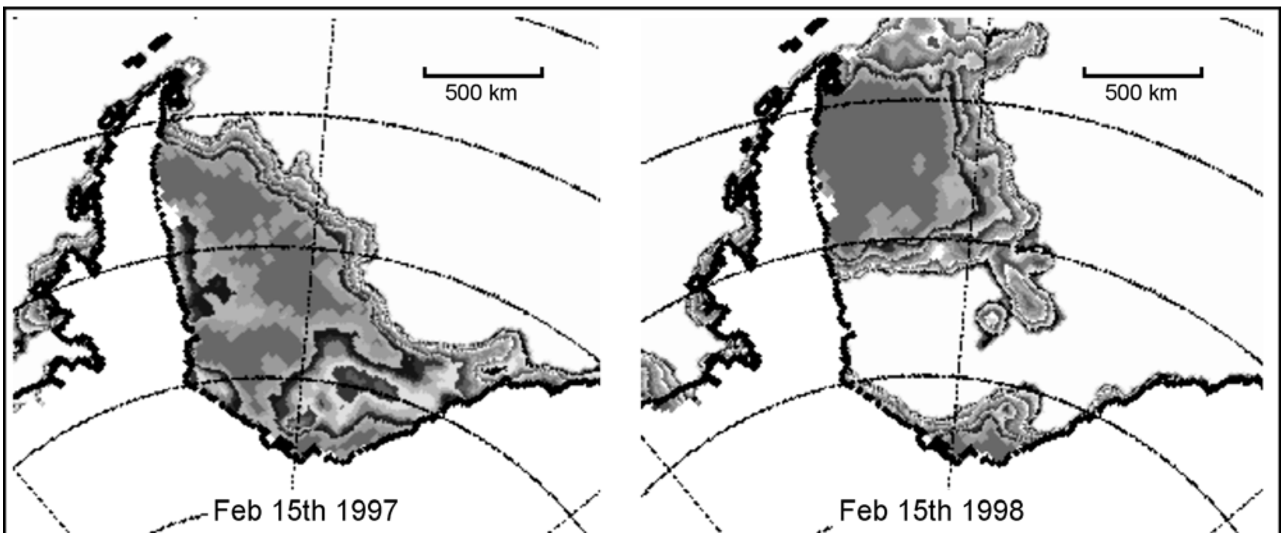

Figure 9. Sea ice coverage over southern Weddell Sea in (left) February 1997 and (right) February 1998.

causing the sea ice to be exported from the continental shelf regime. We suggest that the freezing-up of this expanse of open water at the start of the 1998 winter generated a large pulse of HSSW, the results of which we see in the site 5 time series. This suggestion is subject to the condition that in situ melting of sea ice had not played an important role in creating the anomalous sea ice conditions. Had that been the case the early winter water column would be expected to have an abnormally fresh upper layer, and wintertime freezing would first have to overcome this additional stability before HSSW production could start. However, CTD sections repeated along Ronne Ice Front during several summers show that the 34.40 isohaline, for example, was not abnormally deep in the late austral summer of 1998 [*Nicholls et al.*, 2003; *Gammelsrød et al.*, 1994; *Foldvik et al.*, 1985], supporting *Ackley et al.*'s [2001] finding that the ice was removed from the shelf environment largely as a result of wind forcing, and that there was therefore no abnormal hindrance to the production of HSSW.

[18] We therefore assume that the high currents seen in the first few months of the site 5 time series were driven by the drainage under gravity of the large influx of HSSW. Once the HSSW descended to the depths of the sub-ice shelf cavity, the excess driving disappeared, and the current reduced to its normal strength. The inflowing glut of HSSW traveled round the southern tip of Berkner Island, past site 4 (which was unfortunately not operational at the time of the anomaly), and onward into the Filchner Depression.

[19] According to *Nicholls et al.* [2001] the principal water mass within the enhanced inflow came from the Ronne Depression, and is water too dense to escape the Filchner Depression. It is trapped by topography and, after having traveled along the western slope of Filchner Depression, returns beneath Filchner Ice Front to supply heat to the deep grounding lines. The grounding line in the vicinity of the Foundation Ice Stream (Figure 1) is one such region. It has been suggested [e.g., *Bombosch and Jenkins*, 1995] that basal melting in this region supplies the ISW that ultimately causes the freezing east of Henry Ice Rise. As mentioned above, this is also the region from which ISW is believed to recirculate past site 5. The glut of HSSW from the Ronne Depression has now been converted into a glut of very cold ISW, which presumably continues on to the Filchner Ice Front.

[20] Another major event occurred in the southern Weddell Sea during 1998: the breakout of the eastern portion of Ronne Ice Front. Icebergs A38, A39 and A41 calved from the ice front in the Austral spring of 1998, and drifted over and off the southern continental shelf during the following ten months [*Jung-Rothenhäusler and Oerter*, 2000]. This event is likely to have perturbed cross-ice front flows over Berkner Bank, and to have provided additional ice front length during the period the icebergs remained over the continental shelf. However, it is our contention that the unprecedented size of the 1997–1998 summer polynya would have been the dominant influence on HSSW production during the 1998 winter.

4. Ventilation Timescales

[21] Using the anomalous glut of HSSW as a marker, it is possible to estimate the interval between HSSW entering the cavity beneath the western Ronne Ice Shelf, and the resulting ISW exiting at the Filchner Ice Front, having circulated once around the Filchner Depression. We define this as a "flushing timescale" for the cavity. The time taken to recover fully from the anomaly we define as the "ventilation timescale".

[22] In their modeling studies, *Jenkins et al.* [2004] find two distinct inflows into the Ronne Depression, one during the late winter and the other during the summer. In their model, the summer inflow depends on the strength of freezing during the previous winter, and it is that flow that heads east toward Berkner Island; the winter inflow ventilates mainly the Ronne Depression, and is caused by processes local to the ice front. The strength of the summer inflow is likely to be more affected by the sea-ice extent during the previous summer. Measurements from moorings deployed at the ice front in the Ronne Depression [*Nicholls et al.*, 2003] indicate a late-summer inflow. We assume this to be the inflow that the model runs of *Jenkins et al.* [2004] place in midsummer: the absolute phasing of the modeled seasonality in the runs of *Jenkins et al.* [2004] is not well constrained as the model is driven with a simple sinusoidal sea surface salinity. Given an inflow into the cavity in February 1999 [*Nicholls et al.*, 2003], the total time for the water to travel to the Berkner coast, around the Filchner Depression, and return to site 5 as the pulse of very cold ISW observed in late 2000 is around 22 months.

[23] The route around the Filchner Depression is about 2500 km in length. From Figure 5, the HSSW/ISW appears to complete the journey in around 20 months, suggesting an average speed of about 5 cm s^{-1}. If, after having returned to site 5, the ISW glut travels back to the Filchner Ice Front at about the same speed, we would expect it to make the 700-km journey in about 5 or 6 months. The flushing time for the cavity is therefore of the order of 2–2.5 years. A typical mean speed of flow beneath an ice shelf is unavailable, as so few measurements have been made. At site 3, the mean flow was around 3 to 4 cm s^{-1}, comparable with our value of 5 cm s^{-1} for the circulation within the Filchner Depression. Cross correlating the temperature records from the deepest instruments at sites 4 and 5 shows a delay of 13.5 days between signals at the two sites. The distance the water has to cover is about 140 km, implying an average speed of around 12 cm s^{-1}. Although this is substantially higher than our suggested value for the average for the entire route around the depression, the section of the route lying between the two sites would be expected to be characterized by higher velocities as a result of the steep topography, for example, the >20 cm s^{-1} observed at site 5. Indeed, model runs that resolve the flow past site 5 suggest a deceleration to the south [*Jenkins and Holland*, 2002].

[24] Clearly, we have not calculated a true ventilation time. Full ventilation would require a large fraction of the volume of the cavity to be refreshed. Indeed, even as a transit time for HSSW it is an underestimate, as the speed of propagation of the anomalous glut of HSSW around the cavity would be expected to be anomalously high (Figure 4). For example, during 1999 the temperature peak in the record from the deepest instrument at site 5 occurred 2 to 3 months earlier than during the following three years, implying a somewhat longer flushing time for a "normal" sequence of years. The distance from the Ronne Depression

ice front to site 5 is about 600 km. From the time that we presume the HSSW entered the cavity (February 1999), and the date of arrival of the HSSW glut at site 5 (June 1999), we estimate the average speed of flow between ice front and drill site to be around 6 cm s^{-1}, compared with a "normal" year, when it would be nearer 4 cm s^{-1}. A different approach to obtaining a ventilation time is by simply noting how long the water column at site 5 takes to return to its pre-1999 condition. Unfortunately, we don't have a measurement of that initial condition, and so we approximate the pre-1999 state by the conditions observed at the beginning of the time series (late January 2000). The top panel in Figure 5 shows that, while the deeper part of the water column had recovered within about 18 months, the upper part had only just recovered by the end of the time series, implying a ventilation timescale of 4 to 5 years. A commonly used approximation for ventilation timescales involves simply dividing the cavity volume (1.5×10^{14} m^3) by the estimated influx ($0.9 \pm 0.3 \times 10^6$ m^3 s^{-1}, [*Nicholls et al.*, 2003]), which yields a value of 5.4 ± 2 years. This is consistent with the value obtained from this study, suggesting that site 5 is representative of the responsiveness of the cavity as a whole to external forcing.

5. Summary and Conclusions

[25] The time series from the instruments at site 5 strongly suggest an intimate link between the climatic conditions over the southern Weddell Sea continental shelf and the oceanographic conditions deep beneath Ronne Ice Shelf, hundreds of kilometers from the open sea.

[26] The most likely cause of the nonseasonal signal seen in the first half of the site 5 time series is the unprecedented sea ice conditions over the southern Weddell Sea continental shelf during the 1997–1998 summer. A very large expanse of open water present at the end of the austral summer resulted in a high rate of production of HSSW during the winter freeze-up. In the late summer of 1998–1999 the resulting glut of HSSW entered the cavity via the Ronne Depression at the north western end of the ice front. The HSSW then flowed beneath the ice shelf, toward the west coast of Berkner Island, with its peak arriving at site 5 in June 1999, 2–3 months earlier than the seasonal pulse for a "normal" year. The unusually strong forcing resulted in high mean currents at site 5 until the glut had descended to the deepest parts of the cavity. Over the following 20 months the pulse traveled around the Filchner Depression, trapped by the topography. In early 2001 the glut returned to site 5, this time as a pulse of very cold ISW, having been cooled by melting at the deep grounding lines at the southern reaches of the cavity. The ISW then, presumably, returns to the Filchner Ice Front. From mid-2001 the variability at site 5 appears to return to a regular seasonal cycle.

[27] We estimate the time from HSSW entry into the cavity, to its rearrival as ISW at the Filchner Ice Front after one circuit of the Filchner Depression, to be of the order of 24–30 months. This is a measure of the flushing time of the cavity. We note that the conditions during this period were exceptional, in that the cavity was forced at an unusually high level by the extraordinary sea-ice conditions. It is, however, the first direct measurement of flushing timescales, and it highlights the cavity's responsive nature to external forcing. By noting the length of time the water column at site 5 takes to recover to its pre-1999 state, we estimate a full ventilation time for the cavity of around 4 to 5 years a value significantly lower than previous estimates [*Gammelsrød et al.*, 1994; *Mensch et al.*, 1996].

[28] **Acknowledgments.** The authors are grateful to Keith Makinson and Adrian Jenkins for their helpful comments on the manuscript, and to the reviewers, whose constructive criticisms lead to significant improvements.

References

Ackley, S. F., C. Geiger, J. C. King, E. C. Hunke, and J. C. Comiso (2001), The Ronne polynya of 1997–98: Observations of air-ice-ocean interaction, *Ann. Glaciol.*, *33*, 425–429.
Bombosch, A., and A. Jenkins (1995), Modeling the formation and deposition of frazil ice beneath Filchner-Ronne Ice Shelf, *J. Geophys. Res.*, *100*, 6983–6992.
Carmack, E. C., and T. D. Foster (1975), Circulation and distribution of oceanographic properties near Filchner Ice Shelf, *Deep Sea Res.*, *22*, 77–90.
Foldvik, A., and T. Gammelsrød (1988), Notes on Southern-Ocean hydrography, sea-ice and bottom water formation, *Palaeogeogr. Palaeoclimatol. Palaeoecol.*, *67*, 3–17.
Foldvik, A., T. Gammelsrød, and T. Tørresen (1985), Circulation and water masses on the southern Weddell Sea Shelf, in *Oceanology of the Antarctic Continental Shelf*, *Antarct. Res. Ser.*, vol. 43, edited by S. S. Jacobs, pp. 5–20, AGU, Washington, D. C.
Foldvik, A., T. Gammelsrød, E. Nygaard, and S. Østerhus (2001), Current measurements near Ronne Ice Shelf: Implications for circulation and melting, *J. Geophys. Res.*, *106*, 4463–4477.
Foster, T. D., and E. C. Carmack (1976), Frontal zone mixing and Antarctic Bottom Water formation in the southern Weddell Sea, *Deep Sea Res.*, *23*, 301–317.
Gammelsrød, T., A. Foldvik, O. A. Nøst, Ø. Skagseth, L. G. Anderson, E. Fogelqvist, K. Olsson, T. Tanhua, E. P. Jones, and S. Østerhus (1994), Distribution of water masses on the continental shelf in the southern Weddell Sea, in *The Polar Oceans and Their Role in Shaping the Global Environment*, *Geophys. Monogr. Ser.*, vol. 85, edited by O. M. Johannessen, R. D. Muench, and J. E. Overland, pp. 159–176, AGU, Washington, D. C.
Gerdes, R., J. Determann, and K. Grosfeld (1999), Ocean circulation beneath Filchner-Ronne Ice Shelf from three- dimensional model results, *J. Geophys. Res.*, *104*, 15,827–15,842.
Gordon, A. L. (1998), Western Weddell Sea thermohaline stratification, in *Ocean, Ice and Atmosphere: Interactions at the Antarctic Continental Margin*, *Antarct. Res. Ser.*, vol. 75, edited by S. S. Jacobs and R. F. Weiss, pp. 215–240, AGU, Washington, D. C.
Hunke, E. C., and S. F. Ackley (2001), A numerical investigation of the 1997–1998 Ronne Polynya, *J. Geophys. Res.*, *106*, 22,373–22,382.
Jenkins, A., and C. S. M. Doake (1991), Ice-ocean interaction on Ronne Ice Shelf, Antarctica, *J. Geophys. Res.*, *96*, 791–813.
Jenkins, A., and D. M. Holland (2002), A model study of ocean circulation beneath Filchner-Ronne Ice Shelf, Antarctica: Implications for bottom water formation, *Geophys. Res. Lett.*, *29*(8), 1634, doi:10.1029/2002GL015647.
Jenkins, A., D. M. Holland, K. W. Nicholls, M. Schröder, and S. Østerhus (2004), Seasonal ventilation of the cavity beneath Filchner-Ronne Ice Shelf simulated with an isopycnic coordinate ocean model, *J. Geophys. Res.*, *109*, C01024, doi:10.1029/2001JC001086.
Jung-Rothenhäusler, F., and H. Oerter (2000), Breakaway and movement of Iceberg A38, in *FRISP Report 13*, edited by H. Oerter, Alfred Wegener Inst., Bremerhaven, Germany.
Mensch, M., R. Bayer, J. L. Bullister, P. Schlosser, and R. Weiss (1996), The Distribution of tritium and CFCs in the Weddell Sea during the mid-1980s, *Prog. Oceanogr.*, *38*, 377–415.
Millero, F. J. (1978), Freezing point of sea water, in *Eighth Report of the Joint Panel of Oceanographic Tables and Standards*, Appendix 6, *UNESCO Tech. Pap. Mar. Sci.*, *28*, 29–31.
Nicholls, K. W. (1996), Temperature variability beneath Ronne Ice Shelf, Antarctica, from thermistor cables, *J. Geophys. Res.*, *101*, 1199–1210.
Nicholls, K. W., and K. Makinson (1998), Ocean circulation beneath the western Ronne Ice Shelf, as derived from in situ measurements of water currents and properties, in *Ocean, Ice, and Atmosphere: Interactions at the Antarctic Continental Margin*, *Antarct. Res. Ser.*, vol. 75, edited by S. S. Jacobs and R. F. Weiss, pp. 301–318, AGU, Washington, D. C.
Nicholls, K. W., S. Østerhus, K. Makinson, and M. R. Johnson (2001), Oceanographic conditions south of Berkner Island, beneath Filchner-Ronne Ice Shelf, Antarctica, *J. Geophys. Res.*, *106*, 1481–1492.

Nicholls, K. W., L. Padman, M. Schröder, R. A. Woodgate, A. Jenkins, and S. Østerhus (2003), Water mass modification over the continental shelf north of Ronne Ice Shelf, Antarctica, *J. Geophys. Res.*, *108*(C8), 3260, doi:10.1029/2002JC001713.

Renfrew, I. A., J. C. King, and T. Markus (2002), Coastal polynyas in the southern Weddell Sea: Variability of the surface energy budget, *J. Geophys. Res.*, *107*(C6), 3062, doi:10.1029/2000JC000720.

Williams, M. J. M., A. Jenkins, and J. Determann (1998), Physical controls on ocean circulation beneath ice shelves revealed by numerical models, in *Ocean, Ice, and Atmosphere: Interactions at the Antarctic Continental Margin*, *Antarct. Res. Ser.*, vol. 75, edited by S. S. Jacobs and R. Weiss, pp. 285–299, AGU, Washington, D. C.

K. W. Nicholls, British Antarctic Survey, Natural Environment Research Council, High Cross, Madingley Road, Cambridge CB3 0ET, UK. (kwni@bas.ac.uk)

S. Østerhus, Bjerknes Centre for Climatic Research, University of Bergen, Allegaten 70, N-5007 Bergen, Norway.